

DEEP XVA SOLVER – A NEURAL NETWORK BASED COUNTERPARTY CREDIT RISK MANAGEMENT FRAMEWORK

ALESSANDRO GNOATTO, ATHENA PICARELLI, AND CHRISTOPH REISINGER

May 26, 2022

ABSTRACT. In this paper, we present a novel computational framework for portfolio-wide risk management problems where the presence of a potentially large number of risk factors makes traditional numerical techniques ineffective. The new method utilises a coupled system of BSDEs for the valuation adjustments (xVA) and solves these by a recursive application of a neural network based BSDE solver. This not only makes the computation of xVA for high-dimensional problems feasible, but also produces hedge ratios and dynamic risk measures for xVA, and allows simulations of the collateral account.

1. INTRODUCTION

As a consequence of the 2007–2009 financial crisis, academics and practitioners have been redefining and augmenting key concepts of risk management. This made it necessary to reconsider many widely used methodologies in quantitative and computational finance.

As an example, it is now generally accepted that a reliable valuation of a financial product should account for the possibility of default of any agent involved in the transaction. Moreover, the trading activity is nowadays funded by resorting to different sources of liquidity. This results in the interest rate multi-curve phenomenon that, in such a framework, the existence of a unique funding stream with a unique risk-free interest rate no longer represents a realistic assumption. The increasingly important role of collateral agreements, demands for a portfolio-wide view on valuation.

The aforementioned stylized facts are incorporated at the level of valuation equations by introducing value adjustments (xVA). Value adjustments are further terms to be added to, or subtracted from, an idealized reference portfolio value, computed in the absence of frictions, in order to obtain the final value of the transaction.

The literature on counterparty credit risk and funding is large and we only attempt to provide insights on the main references as they relate to our work. Possibly the first contribution on the subject is a model for credit risk asymmetry in swap contracts in Duffie and Huang (1996). Before the 2007–2009 financial crisis, we have the works of Brigo and Masetti (2005) and Cherubini (2005), where the concept of credit valuation adjustment (CVA) is analyzed. The possibility of default of both counterparties involved in the transaction, represented by the introduction of the debt valuation adjustment (DVA), is investigated, among others, in Brigo et al. (2011) and Brigo et al. (2014).

Another important source of concern for practitioners apart from default risk is represented by funding costs. A parallel stream of literature emerged during and after the financial crisis to generalize valuation equations to include the presence of collateralization agreements. In a Black-Scholes economy, Piterbarg (2010) provides valuation formulas both in the collateralized and uncollateralized case. Generalizations to the case of a multi-currency economy can be found in Piterbarg (2012), Fujii et al. (2010) and Fujii et al. (2011). The funding valuation adjustment (FVA) is derived under alternative

2010 *Mathematics Subject Classification.* 91G30, 91B24, 91B70. *JEL Classification* E43, G12.

Key words and phrases. CVA, DVA, FVA, ColVA, xVA, EPE, Collateral, xVA hedging, Deep BSDE Solver.

assumptions on the Credit Support Annex (CSA) in Pallavicini et al., while Brigo and Pallavicini (2014) also discusses the role of central counterparties in terms of funding costs. A general approach to funding in a semimartingale setting is provided by Bielecki and Rutkowski (2015).

Funding and default risk need to be united in a single risk management framework to account for all possible frictions and their interplay. Contributions in this sense can be found in Brigo et al. (2018) by means of the so-called discounting approach. In a series of papers, Burgard and Kjaer generalize the classical Black-Scholes replication approach to include some of the aforementioned effects, see Burgard and Kjaer (2011b) and Burgard and Kjaer (2011a). A more general backward stochastic differential equation (BSDE) approach is provided by Crépey (2015a), Crépey (2015b), Bichuch et al. (2018a) and Bichuch et al. (2018b). The equivalence between the discounting approach of Brigo and co-authors and the BSDE-based replication approaches is demonstrated in Brigo et al. (2018).

The importance of the topic is reflected in the increasing number of monographs on the subject, with Brigo et al. (2013) an example of an early work. An advanced BSDE-based treatment is presented by Crépey et al. (2014), while detailed analyses of how to construct large hybrid models for counterparty risk simulations are provided in Green (2015), Lichters et al. (2015) and Sokol (2014). Finally, Gregory (2015) provides an accessible introduction to wide-ranging aspects of the topic.

A common fundamental feature of such generalized risk management frameworks is the necessity to adopt a portfolio-wide point of view in order to properly account for risk mitigation benefits arising from diversified positions. Adopting such portfolio-wide models, as is the present market practice in financial institutions, involves high-dimensional joint simulations of all positions within a portfolio.

Commonly used numerical techniques (see for instance Shöftner (2008); Karlsson et al. (2016); Broadie et al. (2015); Joshi and Kwon (2016)) make use of regression approaches, based on a modification of the Least-Squares Monte Carlo approach in Longstaff and Schwartz (2001), to alleviate the high computational cost of fully nested Monte Carlo simulations such as those initially proposed in Gordy and Juneja (2010); Broadie et al. (2011). For an application of adjoint algorithmic differentiation (AAD) to xVA simulation by regression see, for instance, Capriotti et al. (2017); Fries (2019).

An alternative, hybrid, approach to counterparty risk computations is taken in de Graaf et al. (2014), where standard pricing methods are applied to the products in the portfolio and outer Monte Carlo estimators are applied for exposures. Techniques based purely on PDEs generally suffer from the so-called *curse of dimensionality*, a rapid increase of computational cost in presence of high dimensional problems. A PDE approach with factor-based dimension reduction has been proposed in de Graaf et al. (2018). Observe that in the presence of collaterals, a PDE representation for CVA and DVA is not always available.

Presently, in high dimension (i.e., on portfolio level), there are no well established computational methods that have achieved satisfactory results. However, as explained above, such situations are of great practical relevance.

Modern risk-management frameworks demand the use of advanced parallel programming techniques at the heart of software running on high-performance hardware infrastructures. In recent years, thanks to developments such as the introduction of advanced graphics processing units (GPUs), allowing for massive parallel computations, machine learning techniques have witnessed an increasing popularity in different domains. Such methods prove themselves particularly appealing in the context of high-dimensional problems involving large amounts of data.

Of particular interest is the concept of an artificial neural network (ANN). From a mathematical perspective, ANNs are multiple nested compositions of relatively simple multivariate functions. The term deep neural networks refers to ANNs with several interconnected layers. One remarkable property

of ANNs is given in the “Universal Approximation Theorem”, which has been proven in different versions, starting from the remarkable insight of Kolmogorov’s Representation Theorem, Kolmogorov (1956), and the seminal works of Cybenko (1989) and Hornik (1991). In a nutshell, this result states that any continuous function in any dimension can be represented to arbitrary accuracy by means of an ANN. In this context, and building heavily on earlier work of Jentzen et al. (2018), the recent results by Reisinger and Zhang (2019) have proved that deep ANNs can overcome the curse of dimensionality for approximating (nonsmooth) solutions of partial differential equations arising from (open-loop control of) SDEs. A result to the same effect has been shown for heat equations with a zero-order nonlinearity in Hutzenthaler et al. (2018). This is potentially useful in the context of risk management as simple models for CVA can be expressed in this form. For a recent literature survey of applications of neural networks to pricing, hedging and risk management problems more generally we refer the reader to Ruf and Wang (2019).

In this paper, we investigate the application of ANNs to solve high-dimensional BSDEs arising from risk management problems. Indeed, in the classical continuous-time mathematical finance literature the random behavior of the simple financial assets composing a portfolio is typically described by means multi-dimensional Brownian motions and forward stochastic differential equations (SDEs). In this setting, BSDEs naturally arise as a representation of the evolution of the hedging portfolio, where the terminal condition represents the target payoff (see, e.g., El Karoui et al. (1997)). In essence, (numerically) solving a BSDE is equivalent to identifying a risk management strategy.

More precisely, we will consider a discretized version of the BSDE and parametrize the (high dimensional) control (i.e., hedging) process at every point in time by means of a family of ANNs. Once written in this form, BSDEs can be viewed as model-based reinforcement learning problems. The ANN parameters are then fitted so as to minimize a prescribed loss function. Mathematically, this involves an optimization step over a very large number of variables which typically requires the use of stochastic gradient descent-type algorithms.

The line of computational methods we follow has been initiated in the context of high-dimensional nonlinear PDEs, in E et al. (2017) and further investigated in Henry-Labordere (2017) and Fujii et al. (2019), and has led to the so-called Deep BSDE Solver. By way of financial applications, and xVA specifically, a primal-dual extension to the Deep BSDE Solver has been developed in Henry-Labordere (2017) and tested on stylised CVA- and IM(Initial Margin)-type PDEs; the Deep BSDE Solver has also been applied specifically to exposure computations for a Bermudan swaption and a cross-currency swap in She and Greu (2017).

Our approach goes beyond these earlier works in the following regards: we

- formulate a rigorous, generic BSDE model for the dynamics of xVA, including CVA, DVA, FVA and ColVA (collateral valuation adjustment), for a derivative portfolio;
- provide algorithms for the computation of ‘non-recursive’ xVAs (such as CVA and DVA) and ‘recursive’ xVAs by (recursive) application of a Deep BSDE Solver;
- show how the method can be used for the simulation of xVA sensitivities and collateral.

We will refer to our method as Deep xVA Solver. More recently, an xVA strategy based on deep learning regression has been proposed in Crépey et al. (2019); Albanese et al. (2020), exploiting the numerical approach to BSDEs presented in Huré et al. (2020). Different from E et al. (2017), this solver approximates the value function, not the control, by means of an ANN and reconstructs it at each time step by dynamic programming techniques. A comparison of the performance and robustness of the two approaches will require comprehensive testing in industry-relevant settings. We see as a

structural advantage of our algorithm that it directly computes the xVA hedging strategy.

The paper is organized as follows. The financial framework is established in Section 2. In Section 3, after shortly recalling the main features of the deep BSDE solver presented in E et al. (2017), the algorithm for xVA computation is introduced. Numerical results for a selection of test cases are shown in Section 4, while Section 5 concludes.

2. THE FINANCIAL MARKET

We fix a time horizon $T < \infty$ for the trading activity of two agents named the *bank* (B) and the *counterparty* (C). Unless otherwise stated, throughout the paper we assume the bank's perspective and refer to the bank as the *hedger*.

All underlying processes are modeled over a probability space $(\Omega, \mathcal{G}, \mathbb{G}, \mathbb{Q})$, where $\mathbb{G} = (\mathcal{G}_t)_{t \in [0, T]} \subseteq \mathcal{G}$ is a filtration satisfying the usual assumptions (\mathcal{G}_0 is assumed to be trivial). We denote by τ^B and τ^C the *time of default* of the bank and the counterparty, respectively. Specifically, we assume that $\mathbb{G} = \mathbb{F} \vee \mathbb{H}$, where $\mathbb{F} = (\mathcal{F}_t)_{t \in [0, T]}$ is a reference filtration satisfying the usual assumptions and $\mathbb{H} = \mathbb{H}^B \vee \mathbb{H}^C$, with $\mathbb{H}^j = \left(\mathcal{H}_t^j \right)_{t \in [0, T]}$ for $\mathcal{H}_t^j = \sigma(H_u | u \leq t)$, and $H_t^j := 1_{\{\tau^j \leq t\}}$, $j \in \{B, C\}$. We set

$$(2.1) \quad \tau = \tau^C \wedge \tau^B.$$

In the present paper we will extensively make use of the so called *Immersion Hypothesis* (see, e.g., Bielecki and Rutkowski (2004)).

Hypothesis 2.1. *Any local (\mathbb{F}, \mathbb{Q}) -martingale is a local (\mathbb{G}, \mathbb{Q}) -martingale.*

We consider the following spaces:

- $L^2(\mathbb{R}^d)$ is the space of all \mathcal{F}_T -measurable \mathbb{R}^d -valued random variables $X : \Omega \mapsto \mathbb{R}^d$ such that $\|X\|^2 = \mathbb{E} \left[|X|^2 \right] < \infty$.
- $\mathbb{H}^{2, q \times d}$ is the space of all predictable $\mathbb{R}^{q \times d}$ -valued processes $\phi : \Omega \times [0, T] \mapsto \mathbb{R}^{q \times d}$ such that $\mathbb{E} \left[\int_0^T |\phi_t|^2 dt \right] < \infty$.
- \mathbb{S}^2 the space of all adapted processes $\phi : \Omega \times [0, T] \mapsto \mathbb{R}^{q \times d}$ such that $\mathbb{E} \left[\sup_{0 \leq t \leq T} |\phi_t|^2 \right] < \infty$.

2.1. Basic traded assets.

Risky assets. For $d \geq 1$, we denote by S^i , $i = 1, \dots, d$, the *ex-dividend price* (i.e. the price) of risky securities. All S^i are assumed to be càdlàg \mathbb{F} -semimartingales.

Let $W^\mathbb{Q} = \left(W_t^\mathbb{Q} \right)_{t \in [0, T]}$ be a d -dimensional (\mathbb{F}, \mathbb{Q}) -Brownian motion (hence a (\mathbb{G}, \mathbb{Q}) -Brownian motion, thanks to Hypothesis 2.1). We introduce the following coefficient functions:

$$(2.2) \quad \begin{aligned} \mu &: \mathbb{R}_+ \times \mathbb{R}^d \mapsto \mathbb{R}^d, \\ \sigma &: \mathbb{R}_+ \times \mathbb{R}^d \mapsto \mathbb{R}^{d \times d}, \end{aligned}$$

which are assumed to satisfy standard conditions ensuring existence and uniqueness of strong solutions of SDEs driven by the Brownian motion $W^\mathbb{Q}$. The matrix process σ is assumed to be invertible at every point in time. We assume that

$$(2.3) \quad \begin{cases} dS_t = \mu(t, S_t) dt + \sigma(t, S_t) dW_t^\mathbb{Q}, \\ S_0 = s_0 \in \mathbb{R}^d, \end{cases}$$

on $[0, T]$. Note that we are not postulating that the processes S^i are positive.

Throughout the paper we assume that the market is complete for the sake of simplicity.

Cash accounts. Given a stochastic return process $x := (x_t)_{t \geq 0}$, which is assumed bounded from below, right-continuous and \mathbb{F} -adapted, we define the cash account B^x with unitary value at time 0, as the strictly positive continuous processes of finite variation

$$(2.4) \quad B_t^x := \exp \left\{ \int_0^t x_s ds \right\}, \quad t \in [0, T].$$

In particular, $B^x := (B_t^x)_{t \in [0, T]}$ is also continuous and adapted.

Defaultable bonds. Default times are assumed to be exponentially distributed random variables with time-dependent intensity

$$\Gamma_t^j = \int_0^t \lambda_s^j ds, \quad j \in \{B, C\}, \quad t \in [0, T],$$

where λ^j are non-negative measurable bounded deterministic functions such that

$$\int_0^T \lambda_s^j ds < \infty, \quad \forall t \geq 0, \quad j \in \{B, C\}.$$

We introduce two risky bonds with maturity $T^* \leq T$ and rate of return $r^j + \lambda^j$, issued by the bank and the counterparty, with dynamics

$$(2.5) \quad dP_t^j = (r_t^j + \lambda_t^j) P_t^j dt - P_{t-}^j dH_t^j, \quad P_0^j = e^{-\int_0^{T^* \wedge \tau^j} (r_u^j + \lambda_u^j) du}, \quad j \in \{B, C\}.$$

2.2. xVA framework. We consider a family of contingent claims within a portfolio with agreed dividend stream $A^m = (A_t^m)_{t \in [0, T]}$, $m = 1, \dots, M$, and set $\bar{A}_t^m := 1_{\{t < \tau\}} A_t^m + 1_{\{t \geq \tau\}} A_{\tau-}^m$. The value of the single claims within the portfolio, ignoring any counterparty risk or funding issue, that we refer to as *clean values*, are denoted by $(\hat{V}_t^m)_{m=1, \dots, M}$ and satisfy the following FBSDEs, for $m = 1, \dots, M$,

$$(2.6) \quad \begin{cases} -d\hat{V}_t^m = dA_t^m - r_t \hat{V}_t^m dt - \sum_{k=1}^d \hat{Z}_t^{k,m} dW_t^{k,\mathbb{Q}}, \\ \hat{V}_{T^m}^m = 0, \end{cases}$$

which reads, in integral form,

$$(2.7) \quad \hat{V}_t^m := \mathbb{E}^{\mathbb{Q}} \left[B_t^r \int_{(t, T^m]} \frac{dA_u^m}{B_u^r} \middle| \mathcal{F}_t \right], \quad t \in [0, T^m],$$

where r is a collateral rate in an idealized perfect collateral agreement. For simplicity, we restrict ourselves to European-type contracts and write $A_t^m = 1_{\{t = T^m\}} g^m(S_{T^m})$, $T^m \leq T$, for a family of Lipschitz functions g^m , $m = 1, \dots, M$. Then, equation (2.6) reads

$$(2.8) \quad \begin{cases} -d\hat{V}_t^m = -r_t \hat{V}_t^m dt - \sum_{k=1}^d \hat{Z}_t^{k,m} dW_t^{k,\mathbb{Q}}, \\ \hat{V}_{T^m}^m = g^m(S_{T^m}). \end{cases}$$

Observe that the system (2.3) and (2.8) is decoupled, in the sense that the forward equation (2.3) does not exhibit a dependence on the backward component.

We follow here the framework in Biagini et al. (2019), where the portfolio dynamics are stated in the form of a BSDE under the enlarged filtration \mathbb{G} . We set

$$(2.9a) \quad Z_t^k := \sum_{i=1}^d \xi_t^i \sigma^{i,k}(t, S_t), \quad k = 1, \dots, d,$$

$$(2.9b) \quad U_t^j := -\xi_t^j P_{t-}^j, \quad j \in \{B, C\},$$

$$(2.9c) \quad f(t, V, C) := - \left[(r_t^{f,l} - r_t) (V_t - C_t)^+ - (r_t^{f,b} - r_t) (V_t - C_t)^- + (r_t^{c,l} - r_t) C_t^+ - (r_t^{c,b} - r_t) C_t^- \right],$$

where

- ξ^i , $i = 1, \dots, d$, are the positions in risky assets, while ξ^B, ξ^C are the position in the bank and counterparty bond respectively;
- $r^{f,l}, r^{f,b}$ represent unsecured funding lending and borrowing rates;
- $r^{c,l}, r^{c,b}$ denote the interest on posted and received variation margin (collateral);
- C^+ and C^- represent the posted and received variation margin/collateral.

All above processes are assumed to satisfy suitable regularity conditions ensuring existence and uniqueness for a solution to BSDE (2.10) below. Both posted and received collateral are assumed to be Lipschitz functions of the clean value of the derivative portfolio.

We denote by V the *full contract* value, i.e. the portfolio value including counterparty risk and multiple curves. The \mathbb{G} -BSDE for the portfolio's dynamics then has the form on $\{\tau > t\}$

$$(2.10) \quad \begin{cases} -dV_t = \sum_{m=1}^M d\bar{A}_t^m + (f(t, V, C) - r_t V_t) dt - \sum_{k=1}^d Z_t^k dW_t^{k,\mathbb{Q}} - \sum_{j \in \{B,C\}} U_t^j dM_t^{j,\mathbb{Q}}, \\ V_\tau = \theta_\tau(\hat{V}, C), \quad \text{where} \\ \theta_\tau(\hat{V}, C) := \hat{V}_\tau + 1_{\{\tau^C < \tau^B\}}(1 - R^C) (\hat{V}_\tau - C_{\tau-})^- - 1_{\{\tau^B < \tau^C\}}(1 - R^B) (\hat{V}_\tau - C_{\tau-})^+, \end{cases}$$

where $\hat{V}_t := \sum_{m=1}^M \hat{V}_t^m$ and R^B, R^C are two positive constants representing the recovery rate of the bank and the counterparty, respectively.

In their Theorem 3.15, Biagini et al. (2019) show that there exists a unique solution (V, Z, U) for the \mathbb{G} -BSDE (2.10), and the process V assumes the following form on $\{\tau > t\}$:

$$(2.11) \quad V_t = B_t^r \mathbb{E}^{\mathbb{Q}} \left[\sum_{m=1}^M \int_{(t, \tau \wedge T]} \frac{d\bar{A}_u^m}{B_u^r} + \int_t^{\tau \wedge T} \frac{f(u, V, C)}{B_u^r} du + 1_{\{\tau \leq T\}} \frac{\theta_\tau(\hat{V}, C)}{B_\tau^r} \middle| \mathcal{G}_t \right].$$

To prove existence and uniqueness for the \mathbb{G} -BSDE, Biagini et al. (2019) employ the technique introduced by Crépey (2015a) and reformulate the problem under the reduced filtration \mathbb{F} . Stated in such a form, the problem is also more amenable to numerical computations, especially in the case where f and θ do not depend on V , either explicitly, or implicitly through C .

We consider the following \mathbb{F} -BSDE on $[0, T]$:

$$(2.12) \quad \begin{cases} -d\overline{XVA}_t = \bar{f}(\hat{V}_t, \overline{XVA}_t) dt - \sum_{k=1}^d \bar{Z}_t^k dW_t^{k,\mathbb{Q}}, \\ \overline{XVA}_T = 0, \end{cases}$$

where

$$(2.13) \quad \begin{aligned} \bar{f}(\hat{V}_t, \overline{XVA}_t) &:= -(1 - R^C) (\hat{V}_t - C_t)^- \lambda_t^{C,\mathbb{Q}} \\ &\quad + (1 - R^B) (\hat{V}_t - C_t)^+ \lambda_t^{B,\mathbb{Q}} \\ &\quad + (r_t^{f,l} - r_t) (\hat{V}_t - \overline{XVA}_t - C_t)^+ - (r_t^{f,b} - r_t) (\hat{V}_t - \overline{XVA}_t - C_t)^- \\ &\quad + (r_t^{c,l} - r_t) C_t^+ - (r_t^{c,b} - r_t) C_t^- - (r_t + \lambda_t^{C,\mathbb{Q}} + \lambda_t^{B,\mathbb{Q}}) \overline{XVA}_t. \end{aligned}$$

By standard results on BSDEs, see e.g. Delong (2017, Theorem 4.1.3, Theorem 3.1.1), the existence and uniqueness of solutions $(\hat{V}^m, \hat{Z}^m) \in \mathbb{S}^2(\mathbb{R}) \times \mathbb{H}^{2,q \times 1}$, for $m = 1, \dots, M$, and $(\overline{XVA}, \bar{Z}) \in \mathbb{S}^2(\mathbb{R}) \times \mathbb{H}^{2,q \times 1}$

to, respectively, (2.8) and (2.12), holds under the following conditions:

$$\begin{aligned} r^{f,l}, r^{f,b}, r^{c,l}, r^{c,b}, r \text{ are bounded processes;} \\ |\mu(t, x) - \mu(t, x')| + |\sigma(t, x) - \sigma(t, x')| \leq C|x - x'|, \\ |\sigma(t, x)| + |\mu(t, x)| \leq C(1 + |x|), \end{aligned}$$

for any $t \in [0, T]$, $x, x' \in \mathbb{R}^d$, for some constants $C \geq 0$.

The process $\overline{\text{XVA}}$ coincides with the *pre-default* xVA process. Indeed, given the pre-default value process \overline{V} such that $\overline{V}_t 1_{\{\tau > t\}} = V_t 1_{\{\tau > t\}}$, on $\{\tau > t\}$ the solution to (2.10) can be represented as

$$\overline{V}_t = \hat{V}_t - \overline{\text{XVA}}_t.$$

Moreover, defining the process $\tilde{r} = (\tilde{r}_t)_{t \in [0, T]}$ as $\tilde{r} := r + \lambda^{C, \mathbb{Q}} + \lambda^{B, \mathbb{Q}}$, it has been shown in Biagini et al. (2019, Corollary 3.31) that the process $\overline{\text{XVA}}$ admits the representation

$$(2.14) \quad \overline{\text{XVA}}_t = -\overline{\text{CVA}}_t + \overline{\text{DVA}}_t + \overline{\text{FVA}}_t + \overline{\text{CoIVA}}_t,$$

where

$$(2.15) \quad \overline{\text{CVA}}_t := B_t^{\tilde{r}} \mathbb{E}^{\mathbb{Q}} \left[(1 - R^C) \int_t^T \frac{1}{B_u^{\tilde{r}}} (\hat{V}_u - C_u)^- \lambda_u^{C, \mathbb{Q}} du \middle| \mathcal{F}_t \right],$$

$$(2.16) \quad \overline{\text{DVA}}_t := B_t^{\tilde{r}} \mathbb{E}^{\mathbb{Q}} \left[(1 - R^B) \int_t^T \frac{1}{B_u^{\tilde{r}}} (\hat{V}_u - C_u)^+ \lambda_u^{B, \mathbb{Q}} du \middle| \mathcal{F}_t \right],$$

$$(2.17) \quad \begin{aligned} \overline{\text{FVA}}_t &:= B_t^{\tilde{r}} \mathbb{E}^{\mathbb{Q}} \left[\int_t^T \frac{(r_u^{f,l} - r_u) (\hat{V}_u - \overline{\text{XVA}}_u - C_u)^+}{B_u^{\tilde{r}}} du \middle| \mathcal{F}_t \right] \\ &\quad - B_t^{\tilde{r}} \mathbb{E}^{\mathbb{Q}} \left[\int_t^T \frac{(r_u^{f,b} - r_u) (\hat{V}_u - \overline{\text{XVA}}_u - C_u)^-}{B_u^{\tilde{r}}} du \middle| \mathcal{F}_t \right], \end{aligned}$$

$$(2.18) \quad \overline{\text{CoIVA}}_t := B_t^{\tilde{r}} \mathbb{E}^{\mathbb{Q}} \left[\int_t^T \frac{(r_u^{c,l} - r_u) C_u^+ - (r_u^{c,b} - r_u) C_u^-}{B_u^{\tilde{r}}} du \middle| \mathcal{F}_t \right].$$

This representation highlights that the inclusion of different borrowing and lending rates introduces a non-zero funding adjustment which cannot be found independently of the other adjustments. An algorithm to compute all valuations adjustments systematically in the ‘non-recursive’ and ‘recursive’ setting, especially with the view of potentially large portfolios, is the focus of the next sections.

3. THE ALGORITHM

In this section, we describe the algorithm for the computation of valuation adjustments by neural network approximations to the BSDE introduced in the previous section. We start by briefly recalling the main features of the deep BSDE solver in E et al. (2017). Then, we present the application of the solver to valuation adjustments and its extensions to obtain financially important quantities. We first focus on non recursive adjustments, namely CVA and DVA, and then extend the approach to the recursive case. In particular, we propose to use the deep BSDE solver in E et al. (2017) to approximate the dynamics of \hat{V}_u^m , $m = 1, \dots, M$, $u \in [t, T]$, which constitute the portfolio $\hat{V}_u = \sum_{i=1}^M \hat{V}_u^m$. Once the portfolio value has been approximated and resulting collaterals computed, the value of the adjustment can be obtained either by inserting the values in an ‘outer’ Monte Carlo computation (observe that this strategy only works for non recursive adjustments) or applying a second time the deep BSDE solver to (2.12).

3.1. The deep BSDE solver of E et al. (2017). We describe in this section the main ideas leading to the algorithm by E et al. (2017). We consider a general forward-backward stochastic differential equation (FBSDE) framework.

Let $(\Omega, \mathcal{F}, \mathbb{Q})$ be a probability space rich enough to support an \mathbb{R}^d -valued Brownian motion $W^\mathbb{Q} = (W_t^\mathbb{Q})_{t \in [0, T]}$. Let $\mathbb{F} = (\mathcal{F}_t)_{t \in [0, T]}$ be the filtration generated by $W^\mathbb{Q}$, assumed to satisfy the standard assumptions. Let us consider an FBSDE in the following general form:

$$(3.1) \quad X_t = x + \int_0^t b(s, X_s) ds + \int_0^t a(s, X_s)^\top dW_s^\mathbb{Q}, \quad x \in \mathbb{R}^d$$

$$(3.2) \quad Y_t = \vartheta(X_T) + \int_t^T h(s, X_s, Y_s, Z_s) ds - \int_t^T Z_s^\top dW_s^\mathbb{Q}, \quad t \in [0, T],$$

where the vector fields $b : [0, T] \times \mathbb{R}^d \mapsto \mathbb{R}^d$, $a : [0, T] \times \mathbb{R}^d \mapsto \mathbb{R}^{d \times d}$, $h : [0, T] \times \mathbb{R}^d \times \mathbb{R} \times \mathbb{R}^d \mapsto \mathbb{R}$ and $\vartheta : \mathbb{R}^d \mapsto \mathbb{R}$ satisfy suitable assumptions ensuring existence and uniqueness results. We denote by $(X_t^x)_{t \in [0, T]} \in \mathbb{S}^2(\mathbb{R}^d)$ and $(Y_t^y, Z_t)_{t \in [0, T]} \in \mathbb{S}^2(\mathbb{R}) \times \mathbb{H}^{2, q \times 1}$ the unique adapted solution to (3.1) and (3.2), respectively. To alleviate notations, hereafter we omit the dependency on the initial condition x of the process X^x .

The above formulation of FBSDEs is intrinsically linked to the following stochastic optimal control problem:

$$(3.3) \quad \underset{y, Z=(Z_t)_{t \in [0, T]}}{\text{minimise}} \quad \mathbb{E} \left[|\vartheta(X_T) - Y_T^y|^2 \right] \quad \text{subject to (3.1)–(3.2)}.$$

In particular, a solution (Y, Z) to (3.2) is a minimiser of the problem (3.3). A discretized version of the optimal control problem (3.3) is the basis of the deep BSDE solver.

Given $N \in \mathbb{N}$, consider $0 = t_0 < t_1 < \dots < t_N = T$. For simplicity, let us take a uniform mesh with step Δt such that $t_n = n\Delta t$, $n = 0, \dots, N$, and denote $\Delta W_n = W_{t_{n+1}}^\mathbb{Q} - W_{t_n}^\mathbb{Q}$. By an Euler-Maruyama approximation of (3.1)–(3.2), one has

$$(3.4) \quad \tilde{X}_{n+1} = \tilde{X}_n - b(t_n, \tilde{X}_n)\Delta t + a(t_n, \tilde{X}_n)\Delta W_n, \quad \tilde{X}_0 = x,$$

$$(3.5) \quad \tilde{Y}_{n+1}^y = \tilde{Y}_n - h(t_n, \tilde{X}_n, \tilde{Y}_n, \tilde{Z}_n)\Delta t + \tilde{Z}_n^\top \Delta W_n, \quad \tilde{Y}_0^y = y.$$

The core idea of the deep BSDE solver is to approximate, at each time step n , the control process \tilde{Z}_n in (3.5) by using an artificial neural network (ANN). More specifically, in the Markovian setting, Z_t is a measurable function of X_t , which we approximate by an ANN ansatz and carry out the optimisation above over this parametrised form. For this we introduce next a formalism for the description of neural networks.

ANN approximation. We consider artificial neural networks with $\mathcal{L} + 1 \in \mathbb{N} \setminus \{1, 2\}$ layers. Each layer consists of ν_ℓ nodes (also called *neurons*), for $\ell = 0, \dots, \mathcal{L}$. The 0-th layer represents the *input layer*, whereas the \mathcal{L} -th layer is called the *output layer*. The remaining $\mathcal{L} - 1$ layers are called *hidden layers*. For simplicity we set $\nu_\ell = \nu$, $\ell = 1, \dots, \mathcal{L} - 1$. The input and output dimensions are both d in our case.

A feedforward neural network is a function $\varphi^\varrho : \mathbb{R}^d \mapsto \mathbb{R}^d$. A feedforward neural network is defined via the composition

$$x \in \mathbb{R}^d \mapsto \mathcal{A}_\mathcal{L} \circ \varrho \circ \mathcal{A}_{\mathcal{L}-1} \circ \dots \circ \varrho \circ \mathcal{A}_1(x) \in \mathbb{R}^d,$$

where all \mathcal{A}_ℓ , $\ell = 1, \dots, \mathcal{L}$, are affine transformations

$$\mathcal{A}_1 : \mathbb{R}^d \mapsto \mathbb{R}^\nu, \quad \mathcal{A}_\ell : \mathbb{R}^\nu \mapsto \mathbb{R}^\nu, \quad \ell = 2, \dots, \mathcal{L} - 1, \quad \mathcal{A}_\mathcal{L} : \mathbb{R}^\nu \mapsto \mathbb{R}^d,$$

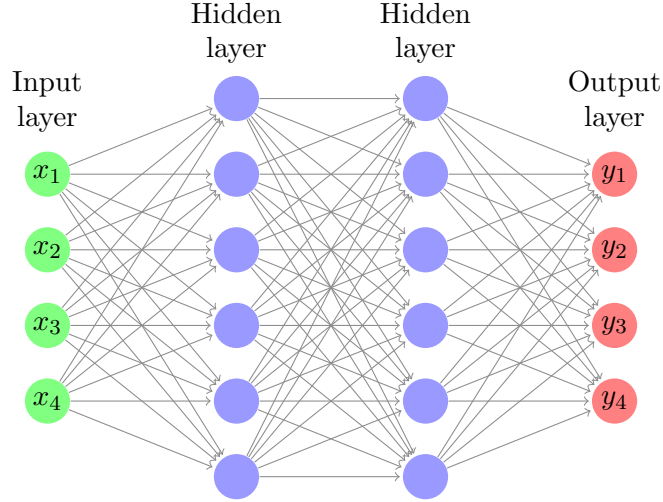


FIGURE 1. Schematic representation of a feedforward neural network with two hidden layers, i.e. $\mathcal{L} = 3$, input and output dimension $d = 4$, and $\nu = d + 2 = 6$ nodes.

of the form $\mathcal{A}_\ell(x) := \mathcal{W}_\ell x + \beta_\ell$, $\ell = 1, \dots, \mathcal{L}$, where \mathcal{W}_ℓ and β_ℓ are matrices and vectors of suitable size called, respectively, weights and biases. The function ϱ , called *activation function* is a univariate function $\varrho : \mathbb{R} \mapsto \mathbb{R}$ that is applied component-wise to vectors. With an abuse of notation, we denote $\varrho(x_1, \dots, x_\nu) = (\varrho(x_1), \dots, \varrho(x_\nu))$. The elements of the weights \mathcal{W}_ℓ and of the vectors β_ℓ are the parameters of the neural network. We can regroup all parameters in a vector $\rho \in \mathbb{R}^R$ where $R = \sum_{\ell=0}^{\mathcal{L}} \nu_\ell(1 + \nu_\ell)$.

As announced we use ANNs to approximate the control process Z_t . More specifically, let $R \in \mathbb{N}$ as before and let $\xi \in \mathbb{R}$, $\rho \equiv (\rho_1, \dots, \rho_R) \in \mathbb{R}^R$ be $R + 1$ parameters. We introduce a family of neural networks $\varphi_n^\rho : \mathbb{R}^d \rightarrow \mathbb{R}^d$, $n \in \{0, \dots, N\}$ parametrized by ρ and indexed by time. We denote $Z_n^\rho = \varphi_n^\rho(X_n)$ and consider the following parametrized version of (3.5)

$$(3.6) \quad Y_{n+1}^{\rho, \xi} = Y_n^{\rho, \xi} - h(t_n, X_n, Y_n^{\rho, \xi}, Z_n^\rho) \Delta t + (Z_n^\rho)^\top \Delta W_n, \quad Y_0^{\rho, \xi} = \xi,$$

meaning that, at each time step, we use a distinct neural network to approximate the control process. The deep BSDE solver by E et al. (2017) considers the following stochastic optimization problem

$$(3.7) \quad \underset{\xi \in \mathbb{R}, \rho \in \mathbb{R}^R}{\text{minimise}} \mathbb{E} \left[\left(\vartheta(X_N) - Y_N^{\rho, \xi} \right)^2 \right] \quad \text{subject to (3.4)–(3.6)}.$$

Observe that, in practice, one simulates $L \in \mathbb{N}$ Monte Carlo paths $(X_n^{(\ell)}, Y_n^{\xi, \rho, (\ell)})_{n=0 \dots N}$ for $\ell = 1, \dots, L$, using (3.4)–(3.6) with N i.i.d. Gaussian random variables $(\Delta W_n)_{n=0, \dots, N-1}$ with mean 0 and variance Δt . Replacing the expected cost functional by the empirical mean, (3.7) becomes

$$(3.8) \quad \underset{\xi \in \mathbb{R}, \rho \in \mathbb{R}^R}{\text{minimise}} \frac{1}{L} \sum_{\ell=1}^L \left(\vartheta(X_T^{(\ell)}) - Y_N^{\rho, \xi, (\ell)} \right)^2 \quad \text{subject to (3.4)–(3.6)}.$$

This minimization typically involves a huge number of parameters and it is performed by a stochastic gradient descent-type algorithm (SGD), leading to random approximations. For further details on this point we refer the reader to Section 2.6 in E et al. (2017). We will denote by \mathcal{I} the maximum number of SGD iterations. To improve the performance and stability of the ANN approximation a *batch normalization* can also be considered, see Ioffe and Szegedy (2015). However, in our framework, this normalization does not always have a positive impact on the results and we will only apply it when resulting in some numerical improvement.

A rigorous and complete theoretical convergence framework for the deep BSDE solver is not available to date. Interesting a posteriori error bounds can be found in Han and Long (2018, Theorem 1'), where the authors show that under suitable assumption on the coefficients of the FBSDE (3.1)-(3.2) (namely the monotonicity of b and h , the Lipschitz continuity in space, Hölder continuity in time, linear growth of b, a, h and the Lipschitz continuity of ϑ) one has, for Δt sufficiently small,

$$(3.9) \quad \sup_{t \in [0, T]} \mathbb{E} |Y_t^y - \tilde{Y}_t^{\rho, \xi}|^2 + \int_0^T \mathbb{E} |Z_t - \tilde{Z}_t^\rho|^2 dt \leq C \left(\Delta t + \mathbb{E} \left[\left(\vartheta(X_N) - Y_N^{\rho, \xi} \right)^2 \right] \right),$$

where C is a constant independent of Δt and d possibly depending on the starting point of the forward process and, given $(Y_n^{\rho, \xi})_{n=0, \dots, N}$ from (3.6), $\tilde{Y}_t^{\rho, \xi} = Y_n^{\rho, \xi}$ and $\tilde{Z}_t^\rho = Z_n^\rho$ for $t \in [t_n, t_{n+1})$.

In Han and Long (2018, Theorem 2'), a priori estimates on the term $\mathbb{E}[(\vartheta(X_N) - Y_N^{\rho, \xi})^2]$ are also provided. However, the obtained bounds depend on the (unknown) approximation capacity of the considered ANN. To corroborate this idea, we mention that in our numerical tests we experienced important variability of results depending on the different structure of the ANN used (see also the results in Figure 5).

3.2. The Deep xVA Solver for non recursive valuation adjustments. In our setting, the deep BSDE solver is first employed in the approximation of the clean values of the portfolio, i.e., the processes \hat{V}_t^m for $m = 1, \dots, M$, which are the solutions of (2.8) with underlying forward dynamics given by S in (2.3). More precisely, in the notation of the previous section, we take

$$X_t = S_t \quad \text{and} \quad Y_t = \hat{V}_t^m \quad \text{for } m = 1, \dots, M.$$

We now describe the algorithm for computing CVA and DVA given by formulas (2.15) and (2.16), respectively. A unifying formula for CVA and DVA can be written as

$$(3.10) \quad B_t^{\tilde{r}} \mathbb{E}^{\mathbb{Q}} \left[\int_t^T \Phi(u, \hat{V}_u) du \middle| \mathcal{F}_t \right],$$

where

- $\Phi(u, v) = (1 - R^C) \frac{1}{B_u^{\tilde{r}}} (v - C_u)^- \lambda_u^{C, \mathbb{Q}}$ for CVA;
- $\Phi(u, v) = (1 - R^B) \frac{1}{B_u^{\tilde{r}}} (v - C_u)^+ \lambda_u^{B, \mathbb{Q}}$ for DVA.

Given a time discretization (uniform, for simplicity) with time step Δt , the integral in (3.10) can be approximated by a quadrature rule, i.e.

$$\int_0^T \Phi(u, \hat{V}_u) du \approx \sum_{n=0}^N \eta_n \Phi(t_n, \hat{V}_{t_n}).$$

For instance, taking $t = t_0 = 0$, one may consider the trapezoidal rule

$$\int_0^T \Phi(u, \hat{V}_u) du \approx \sum_{n=1}^N \frac{\Delta t}{2} (\Phi(t_n, \hat{V}_{t_n}) + \Phi(t_{n-1}, \hat{V}_{t_{n-1}})).$$

Denoting for any $m = 1, \dots, M$ by $(\mathcal{V}_n^{m, \bar{\rho}, \bar{\xi}, (p)})_{n=0, \dots, N, p=1, \dots, P}$ the approximation of the process $(\hat{V}_{t_n}^m)_{n=0, \dots, N}$ obtained by means of the parameters $(\bar{\rho}, \bar{\xi})$ resulting from the deep BSDE solver optimization (3.7), the adjustment is then approximated by the following formula:

$$\frac{1}{P} \sum_{p=1}^P \left(\sum_{n=0}^N \eta_n \Phi(t_n, \sum_{m=1}^M \mathcal{V}_n^{m, \bar{\rho}, \bar{\xi}, (p)}) \right).$$

Algorithms 1 and 2 summarize the main steps of the method.

Algorithm 1: Deep algorithm for exposure simulation

Set parameters: N, L . $\triangleright N$ time steps, L paths for inner Monte Carlo loop
 Fix architecture of ANN. \triangleright intrinsically defines the number of parameters R
Deep BSDE solver (N, L) :
 Simulate L paths $(S_n^{(\ell)})_{n=0, \dots, N}$, $\ell = 1, \dots, L$ of the forward dynamics.
 Define the neural networks $(\varphi_n^\rho)_{n=1, \dots, N}$.
for $m = 1, \dots, M$ **do**
 Minimize over ξ and ρ

$$\frac{1}{L} \sum_{\ell=1}^L \left(g^m(S_N^{(\ell)}) - \mathcal{V}_N^{m, \rho, \xi, (\ell)} \right)^2,$$

subject to

$$(3.11) \quad \begin{cases} \mathcal{V}_{n+1}^{m, \rho, \xi, (\ell)} = \mathcal{V}_n^{m, \rho, \xi, (\ell)} - f(t_n, S_n^{(\ell)}, \mathcal{V}_n^{m, \rho, \xi, (\ell)}, \mathcal{Z}_n^{\rho, (\ell)}) \Delta t + (\mathcal{Z}_n^{\rho, (\ell)})^\top \Delta W_n^{(\ell)}, \\ \mathcal{V}_0^{m, \rho, \xi, (\ell)} = \xi, \\ \mathcal{Z}_n^{\rho, (\ell)} = \varphi_n^\rho(S_n^{(\ell)}). \end{cases}$$

Save the optimizer $(\bar{\xi}^m, \bar{\rho}^m)$.
end
end

Algorithm 2: Deep xVA Solver for non recursive valuation adjustments

Apply Algorithm 1
 Set parameters: P . $\triangleright P$ paths for the outer Monte Carlo loop
 Simulate, for $m = 1, \dots, M$, $(\mathcal{V}_n^{m, (p)})_{n=0, \dots, N, p=1, \dots, P}$ by means of (3.11) with $\xi = \bar{\xi}^m$, $\rho = \bar{\rho}^m$.
 \triangleright approximation of the clean values
 Define $\mathcal{V}_n^{(p)} := \sum_{m=1}^M \mathcal{V}_n^{m, (p)}$ for $n = 0, \dots, N$, $p = 1, \dots, P$.
 \triangleright approximation of the clean portfolio value
 Compute the adjustment as

$$\frac{1}{P} \sum_{i=1}^P \left(\sum_{n=0}^N \eta_n \Phi(t_n, \mathcal{V}_n^{(p)}) \right).$$

Estimates (3.9) can be used to obtain a posteriori bounds on the L^2 error for exposures in $[0, T]$ starting from the loss function, however, the MC error should be added to obtain a computable bound.

3.3. The Deep xVA Solver for recursive valuation adjustments. The procedure of the previous section is sufficient to perform the estimation of CVA and DVA according to (2.15) and (2.16) at time zero by means of a standard Monte Carlo estimator, given the pathwise solutions of the BSDEs for clean values. Typically, however, the bank needs to also compute risk measures on the CVA, such as Value-at-Risk. Also, if we look at the driver of the xVA BSDE (2.12) we observe that FVA terms introduce a recursive structure in the driver, so that even a time t estimate of the process \overline{XVA} requires the use of a numerical solver for a BSDE. Finally, let us observe that the bank is not only interested in computing the xVA at time t , also hedging the market risk of xVA is important, meaning that one also needs sensitivities of valuation adjustments with respect to the driving risk factors.

All above considerations motivate us to propose a two-step procedure, where we first employ the deep BSDE solver to estimate the clean values \hat{V}^m , $m = 1, \dots, M$, according to Algorithm 1 and then, using the simulated paths of the M clean BSDEs obtained from the first step, we apply again the deep BSDE solver to numerically solve the xVA BSDE (2.12). The procedure is outlined in Algorithm 3.

Algorithm 3: Deep xVA Solver

Apply Algorithm 1.

Set parameters: P . $\triangleright P$ paths for outer Monte Carlo loop

Fix architecture of ANN.

 \triangleright intrinsically defines the number of parameters \bar{R} (in general $\bar{R} \neq R$)**Deep XVA-BSDE solver** (N, P):Simulate P paths $(\mathcal{V}_n^{(p)})_{n=0, \dots, N}$, $p = 1, \dots, P$, of the portfolio value.Define the neural networks $(\psi_n^\zeta)_{n=1, \dots, N}$.Minimize over γ and ζ

$$\frac{1}{P} \sum_{p=1}^P \left(\mathcal{X}_N^{\zeta, \gamma, (p)} \right)^2,$$

subject to

$$(3.12) \quad \begin{cases} \mathcal{X}_{n+1}^{\zeta, \gamma, (p)} = \mathcal{X}_n^{\zeta, \gamma, (p)} - \bar{f}(\mathcal{V}_n^{(p)}, \mathcal{X}_n^{\zeta, \gamma, (p)}) \Delta t + (\bar{Z}_n^{\zeta, (p)})^\top \Delta W_n^{(p)}, \\ \mathcal{X}_0^{\zeta, \gamma, (p)} = \gamma, \\ \bar{Z}_n^{\zeta, (p)} = \psi_n^\zeta(\mathcal{V}_n^{(p)}). \end{cases}$$

end

3.4. Pathwise simulation of sensitivities. One interesting feature of our approach to xVA computations is that we can easily estimate several sensitivities (i.e., partial derivatives) of pricing functions. Let us recall that, in the present Markovian setting, the control Z associated to a FBSDE of the general form (3.1)–(3.2) satisfies

$$(3.13) \quad Z_t = \frac{\partial Y}{\partial X}(t, X_t) a(t, X_t),$$

so that we can easily reconstruct the gradient of the pricing function with respect to all risk factors simply by multiplying each (vector-valued) neural network by the inverse (which is assumed to exist) of the matrix $a(t, X_t)$. This becomes particularly interesting in view of Algorithms 1 and 3, where we can obtain hedge ratios both for the clean value and for the valuation adjustments without further computations.

Obtaining second order sensitivities, which may also be important for hedging purposes, is also feasible in our setting, because feedforward neural networks are compositions of simple functions and computation of gradients of neural network functions has become standard in that community. Using the notation of Section 3.1, we can write

$$(3.14) \quad \frac{\partial Z_n^\rho}{\partial X_n} = \frac{\partial \varphi^\rho(X_n)}{\partial X_n},$$

with $\varphi^\rho(X_n) = \mathcal{A}_\mathcal{L}(\rho(\mathcal{A}_{\mathcal{L}-1} \dots \rho(\mathcal{A}_1(X_n))))$. Since $(\mathcal{A}_\ell)_{\ell=1, \dots, \mathcal{L}}$ are affine functions, their Jacobians are given by the weight matrices, i.e.

$$J_{\mathcal{A}_\ell}(\cdot) = \mathcal{W}_\ell, \quad \ell = 1, \dots, \mathcal{L}.$$

Moreover, one also has the Jacobian of ρ ,

$$J_\rho(\cdot) = \text{diag}(\rho'(\cdot)),$$

where, for $x \in \mathbb{R}^\nu$ we denote $\varrho'(x) = (\varrho'(x_1), \dots, \varrho'(x_\nu))$. In the present paper, we choose $\varrho(x) = \text{ReLU}(x) = \max\{x, 0\}$ so that the first derivative can be defined as

$$\varrho'(x) = \text{ReLU}'(x) = \left\{ \begin{array}{ll} 1 & \text{if } x > 0 \\ 0 & \text{otherwise} \end{array} \right\} = \text{sgn}(\text{ReLU}(x)).$$

Finally, we deduce that the following explicit differentiation formula holds:

$$\frac{\partial Z_n^\rho}{\partial X_n} = \mathcal{W}_{\mathcal{L}} \text{diag}(\varrho'(\mathcal{A}_{\mathcal{L}-1}(\dots \mathcal{A}_1(X_n)))) \dots \text{diag}(\varrho'(\mathcal{A}_1(X_n))) \mathcal{W}_1.$$

Given the availability of the derivative of Z_n^ρ we can then obtain the Hessian of Y from (3.13).

4. NUMERICAL RESULTS

To test our algorithm, we start by studying two very simple examples with a similar computational structure as CVA and DVA, and for which we can easily provide reference solutions. We will then give a higher-dimensional example and illustrate further practically relevant features of the method, such as recursive xVA computations and simulation of the collateral account.

Let S be the price of a single stock described by a Black-Scholes dynamics,

$$dS_t = rS_t dt + \sigma S_t dW_t^{\mathbb{Q}}, \quad S_0 = s_0,$$

and \hat{V} a European-style contingent claim with value

$$\hat{V}_t = \mathbb{E} \left[e^{-r(T-t)} g(S_T) \middle| \mathcal{F}_t \right].$$

In particular, \hat{V} solves the following BSDE:

$$(4.1) \quad \begin{cases} -d\hat{V}_t = -r\hat{V}_t dt - Z_t dW_t^{\mathbb{Q}}, \\ \hat{V}_T = g(S_T). \end{cases}$$

The discounted positive and negative expected exposure of \hat{V} are defined, respectively, by

$$(4.2) \quad \text{DEPE}(s) = \mathbb{E}^{\mathbb{Q}} \left[e^{-r(s-t)} \left(\hat{V}_s \right)^+ \middle| \mathcal{F}_t \right],$$

$$(4.3) \quad \text{DENE}(s) = -\mathbb{E}^{\mathbb{Q}} \left[e^{-r(s-t)} \left(\hat{V}_s \right)^- \middle| \mathcal{F}_t \right].$$

In the plots below, we show some promising results obtained from particular realisations of the Deep xVA Solver. A more careful evaluation of the numerical results should also take into account the randomness of the algorithm (through the inner and outer Monte Carlo estimation and stochastic gradient descent).

4.1. A forward on S . In this case we consider

$$g(S_T) = S_T - K$$

with $K = s_0$. The pathwise exposure \hat{V} at time $s \in [t, T]$ is given by

$$\hat{V}_s = \mathbb{E}^{\mathbb{Q}} \left[e^{-r(T-s)} (S_T - K) \middle| \mathcal{F}_s \right] = S_s - K e^{-r(T-s)}.$$

Substituting in (4.2) one has

$$(4.4) \quad \text{DEPE}(s) = S_t \Phi(d_1) - K e^{-r(T-t)} \Phi(d_2),$$

$$(4.5) \quad \text{DENE}(s) = S_t \Phi(-d_1) - K e^{-r(T-t)} \Phi(-d_2),$$

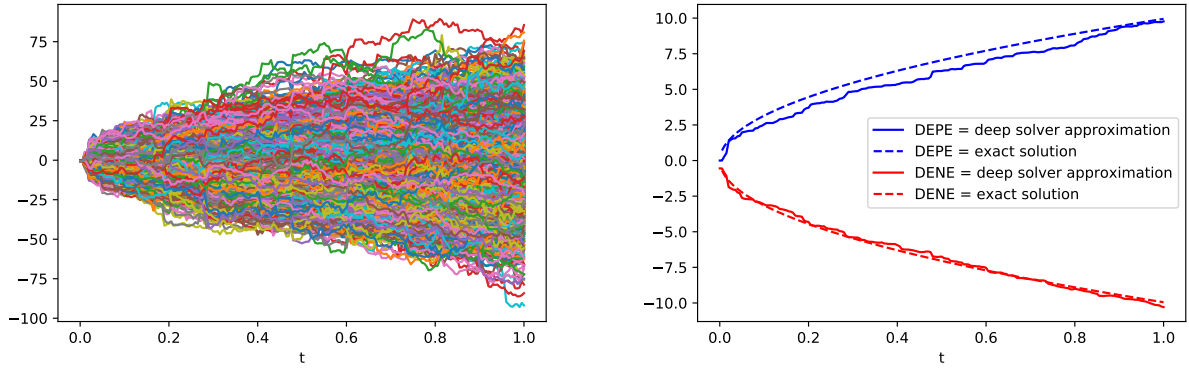


FIGURE 2. Forward contract: approximated exposure (left) and EPE, ENE (right). Parameters used: outer MC paths $P = 2048$, inner MC paths $L = 64$, internal layers $\mathcal{L} - 1 = 2$, $\nu = d + 20 = 21$, $\mathcal{I} = 4000$, time steps $N = 200$, no batch normalization.

where $\Phi(\cdot)$ denotes the standard normal cumulative distribution function and, as usual,

$$d_1 = \frac{\ln(e^{r(t-s)} S_t/K) + (r + \sigma^2/2)(s-t)}{\sigma\sqrt{s-t}} \quad \text{and} \quad d_2 = d_1 - \sigma\sqrt{s-t}.$$

σ	K	T
0.25	100	1

TABLE 1. Parameters used in numerical experiments.

We report in Figure 2 the plot of the numerical results obtained by Algorithm 2 using the parameters in Table 1 and $r = 0$. In particular, on the left we plot the simulated pathwise exposure, i.e. the paths $t_n \rightarrow \mathcal{V}_n^{(p)}$ for $p = 1, \dots, P$, while on the right we compare the approximated EPE and ENE (solid lines) with the exact expected exposures given by (4.4)–(4.5) (dashed lines).

4.2. A European call option. In this case we consider

$$g(S_T) = (S_T - K)^+,$$

where we set $K = s_0$. The pathwise exposure \hat{V} at time $s \in [t, T]$ is given by the Black-Scholes formula

$$\hat{V}_s = \mathbb{E}^{\mathbb{Q}} \left[e^{-r(T-s)} (S_T - K)^+ \middle| \mathcal{F}_s \right] = S_s \Phi(d_1) - K e^{-r(T-s)} \Phi(d_2) > 0.$$

It follows immediately that

$$\text{DEPE}(t) = \mathbb{E}^{\mathbb{Q}} \left[e^{-r(s-t)} \hat{V}_s \middle| \mathcal{F}_t \right] = \hat{V}_t,$$

and

$$\text{DENE}(t) = 0.$$

The results obtained using Algorithm 2 with the parameters in Table 1 and $r = 0.01$ are reported in Figure 3 (left). The exact European call price is 10.40, while the approximation of the exposure obtained by the solver and reported in Figure 3(left) takes values, for $t \in [0, T]$, within the interval $[10.31, 10.33]$ with maximum distance 0.09 to the exact solution.

4.3. A basket call option. Let us now consider the case of several underlying assets (S^1, \dots, S^d) :

$$dS_t^i = r^i S_t^i dt + \sigma^i S_t^i dW_t^{\mathbb{Q}, i}, \quad S_0 = s_0^i \in \mathbb{R}^d, \quad i = 1, \dots, d,$$

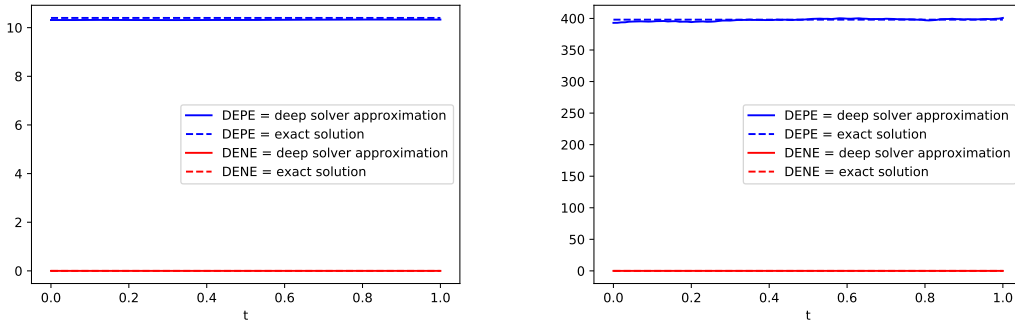


FIGURE 3. DEPE and DENE for a European call option (left) and a European basket option with 100 underlyings (right). Parameters used: outer MC paths $P = 1024$, inner MC paths $L = 64$, internal layers $\mathcal{L} - 1 = 2$, $\nu = d + 20 = 21$ (left) and $\nu = d + 10 = 110$ (right), $\mathcal{I} = 4000$, time steps $N = 100$, with batch normalization.

where $W^{\mathbb{Q}} = (W^{\mathbb{Q},1}, \dots, W^{\mathbb{Q},d})$ is a standard Brownian motion in \mathbb{R}^d with correlation matrix $(\rho_{i,j})_{1 \leq i,j \leq d}$. We set $d = 100$. A European basket call option is associated with the payoff

$$g(S_T^1, \dots, S_T^d) = \left(\sum_{i=1}^d S_T^i - K \right)^+.$$

The results obtained by Algorithm 2 using the parameters in Table 1 with $\sigma^i = \sigma$ for all $i = 1, \dots, d$, zero correlation, and $r^i = r = 0.01$ are reported in Figure 3 (right).

The distinctive feature of the present example is the high dimension of the vector of risk factors. While the two previous one-dimensional examples mainly served as a validation for the methodology, the present example highlights the ability of the proposed methodology to provide an accurate numerical approximation in a high-dimensional context. For this example, we used the feedforward neural network with two layers and $d + 10$ nodes, with a ReLU activation function. The approximation parameters used are reported in the caption of Figure 3 (right). We increase the number of nodes ν roughly linearly with the dimension d , which turned out to be a useful rule-of-thumb for consistent accuracy across dimensions in this case.

A detailed study of deep learning values of basket derivative (on six underlying assets) from simulated values, not based on BSDEs, see Ferguson and Green (2018).

For the case of the basket call option, we observe that the exposure profile corresponds to the present value of the contract. As a consequence, we obtain a simple method to validate the exposure profile by computing an estimate of the basket call option price by means of a standard Monte Carlo simulation with 10^6 paths. We regard this as the ‘exact’ price. The Monte Carlo price we obtained is 398.08 with confidence interval [397.61, 398.56]. The values of the exposure produced by the deep solver reported in Figure 3(right) vary with time between the two values 393.02 and 400.82, achieving the maximum distance 5.06 to the Monte Carlo price at time $t = 0$.

For this product we also perform an xVA calculation with the objective to validate Algorithm 2 and Algorithm 3 in a case where both are applicable. To perform this comparison, we need the xVA BSDE to be non-recursive: this can be achieved by assuming that there is a unique risk-free interest rate, so that FVA and ColVA are identically zero, i.e., xVA consists only of the CVA and DVA term. The idea is then to compare a Monte Carlo estimate of xVA according to Algorithm 2 with the initial value of the BSDE as produced by a full application of Algorithm 3.

We assume that the default intensities of the bank and the counterparty are $\lambda^{C,\mathbb{Q}} = 0.10$ and $\lambda^{B,\mathbb{Q}} = 0.01$, respectively. For the recovery rates we set $R^C = 0.3$ and $R^B = 0.4$, while the unique risk-free interest rate is $r = 0.01$. Using the same network setting (see again the caption of Figure 3, right), the Deep xVA Solver produced an xVA estimate of 208.55 by means of Algorithm 3, whereas the estimate produced by Algorithm 2 is 211.37.

4.4. Realistic simulation of the collateral account. A useful feature of our proposed approach consists in the possibility of performing realistic simulations of the collateral account without resorting to simplifying assumptions. We can in fact compute the overall outstanding exposure between the bank and the counterparty by the following steps. Algorithm 1 allows us to simulate paths for all processes \hat{V}^m , $m = 1, \dots, M$. Such paths can then be aggregated so as to produce a simulation of the portfolio process $\hat{V} = \sum_{m=1}^M \hat{V}^m$, that corresponds to the *pre-collateral exposure*. After this, we compute the value of the collateral balance C corresponding to the simulated paths of \hat{V} , which in turn allows us to compute the *post-collateral exposure* process $\hat{V} - C$ that enters the xVA formulas. For illustration, we consider $M = 1$ and the equity forward from the first example. We introduce a simple example of a collateral agreement where collateral is exchanged between the counterparties at every point in time (a margin call frequency that does not coincide with the simulation time discretization can of course be treated as well). Collateral is exchanged only in case the pre-collateral exposure is above (below) a receiving (posting) threshold which are both set equal to 5, i.e.

$$C_t := C(\hat{V}_t) = (\hat{V}_t - 5)^+ - (\hat{V}_t + 5)^-.$$

An illustration for a single path is provided in Figure 4.

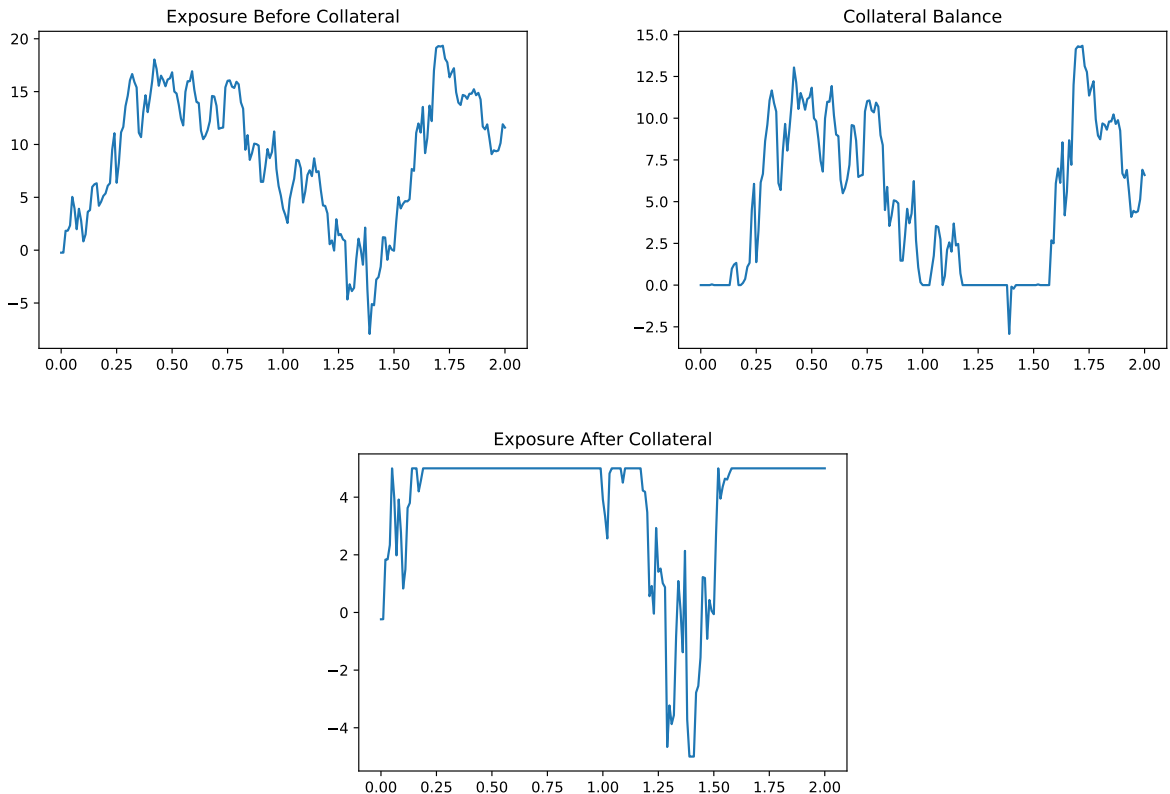


FIGURE 4. Pathwise simulation of a collateralized exposure. The top left panel: \hat{V} . Top right panel C . Bottom panel $\hat{V} - C$. Posting and receiving threshold are 5 EUR.

4.5. Impact of number of layers and nodes. The aim of this section is to analyse the impact of number of nodes and layers of the neural network on the quality of the approximation in our setting. When considering the richness of the network, one can face two adverse, albeit opposite, situations, which are abundantly documented in the literature for various applications: on the one hand, choosing an overly simplistic structure implies that the model *underfits*, i.e., has a poor explanatory capability; on the other hand, a network architecture that is too rich might result in a limited capability of the model to generalize when simulating new paths of the risk factors. This second situation is usually termed *overfitting*.

To analyse the issue in the present setting, we consider the forward contract from Section 4.1 and apply Algorithm 1 to estimate the exposure of the contract. In this case, there is only one risk factor, namely the stock price, so that $d = 1$. We test neural networks with different depths, from one to hidden three layers, and different numbers of nodes, between d and $d + 20$ per layer. A graphical representation of the results is provided in Figure 5. We can clearly observe that a single (non-deep) neural network does not succeed in providing a satisfactory fit to the data, while including more nodes can improve the fit. A two layer network provides the best explanatory capability, with the best results being provided by a 2-layer configuration with $d + 20$ nodes. Adding a further layer, for this particular example, does not lead to an improvement of the fitting quality as testified by the last line of Figure 5, which further shows that adding more nodes has a detrimental effect.

5. PRELIMINARY CONCLUSIONS AND EXTENSIONS

The proposed xVA algorithm exploits two useful complementary aspects of the Deep BSDE Solver of E et al. (2017). First, the formulation as an optimisation problem over a parametrisation of the (Markovian) control of the xVA BSDE, which is carried out by SDE discretisation and path sampling, directly gives both the hedge ratios in approximate functional form and model-based derivative prices along the sample paths. This is amenable to the simulation of exposure profiles, the computation of higher-order Greeks by pathwise differentiation, and allows for the computation of funding and margin variation adjustments as well as xVA hedging. A second aspect of the Deep BSDE Solver is the use of neural networks specifically as parametrisation for the Markovian control. A key advantage results from the approximation power of neural networks in high dimensions, which has the potential to make risk management computations on portfolio level feasible. Moreover, the simple functional form allows standard pathwise sensitivity computations.

Our numerical examples provide a proof of concept, but further systematic testing in realistic application settings is needed. While the basket option example gave good accuracy in a high-dimensional application, we encountered delicate issues with fitting the ANN even for the simple forward contract. An additional difficulty arises from the non-linear, non-convex parametric form, which, combined with the large number of parameters, leads to challenging optimisation problems. Both these aspects, the expression power of the ANN and the practicalities of the learning process, are extremely active research areas and further developments of the proposed Deep xVA Solver will be informed by the rapidly developing understanding of neural networks in a broader sense.

The application of our proposed scheme is not restricted to the chosen xVA framework. For example, one could in principle apply our methodology to the balance-sheet based model computed in Crépey et al. (2019); Albanese et al. (2020). In this case, the xVA computation involves multiple recursive valuations (illustrated succinctly in Abbas-Turki et al. (2018, Figure 1)), which can be approached by means of multiple applications of the Deep xVA Solver.

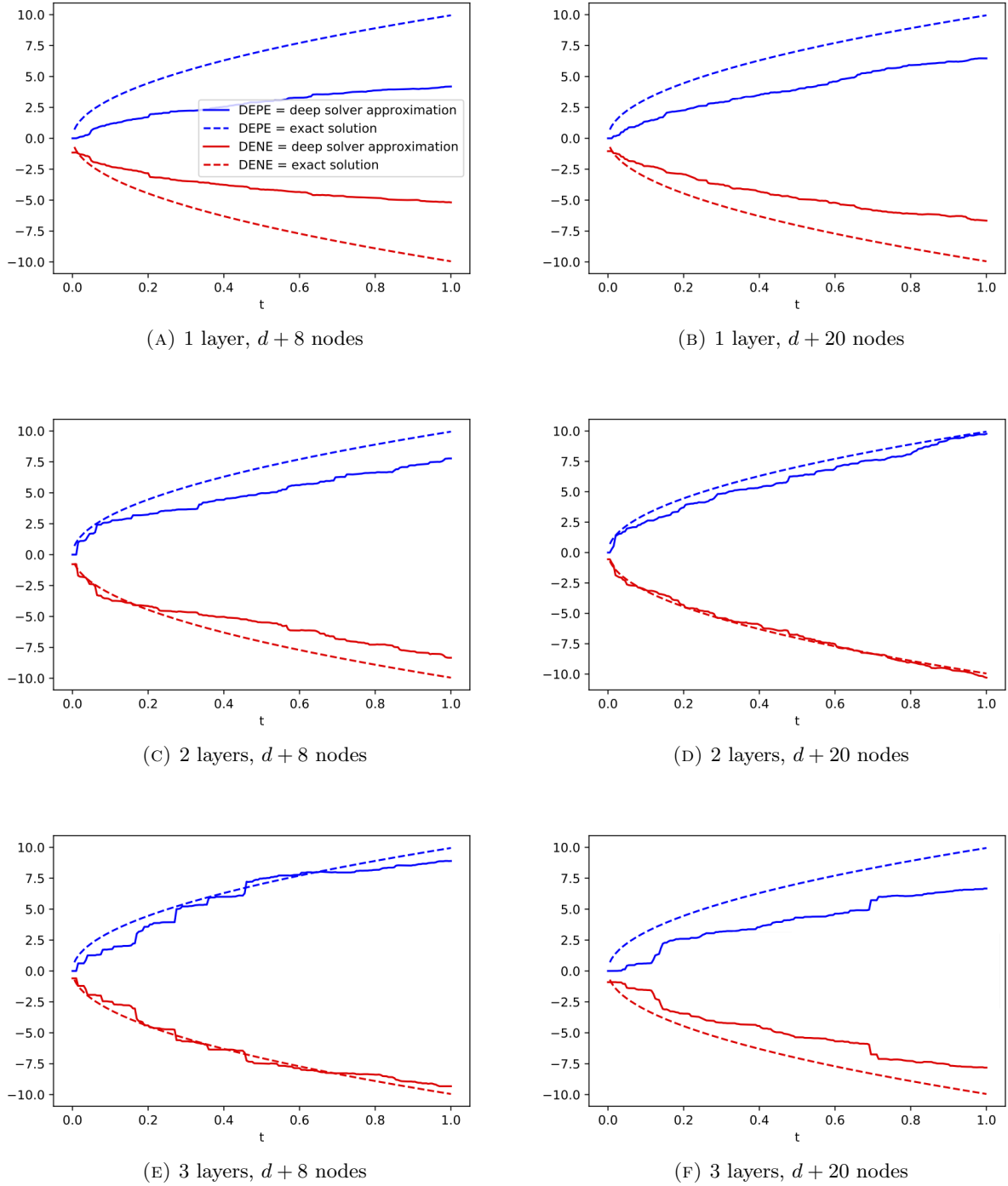


FIGURE 5. Estimation of the exposure for the forward from Example 4.1 obtained with 200 time steps and different numbers of layers and nodes. From the top to bottom: results obtained with 1, 2, 3 layers with $d + 8$ (left) and $d + 20$ (right) nodes.

We also emphasise that the Deep xVA Solver can be combined with an existing analytics library: the computation of the mark-to-market cube (i.e., the simulation of all possible scenarios for the clean values over different points in time) represents a classical numerical problem to be solved in order to compute traditional risk figures such as Value-at-Risk or Expected Shortfall (this is often referred to as “Monte Carlo full revaluation approach”). Since most products individually depend on a limited

number of risk factors, it may be best to use a traditional numerical scheme, such as a finite difference solver, for at least some of the more vanilla products, and then reevaluate the products over different Monte Carlo paths by means of a look-up table over the pre-computed numerical solution. This provides an alternative route with respect to our Algorithm 1 for the simulation of the clean values. However, once we aggregate all mark-to-markets, we end up with an object that depends on a high number of risk factors, so for the computation of xVA our proposed methodology provides a useful tool which allows the recursive computation of valuation adjustments, their hedging strategy, and simulation of collateral.

REFERENCES

- Abbas-Turki, L. A., Crépey, S., and Diallo, B. (2018). XVA principles, nested Monte Carlo strategies, and GPU optimizations. *International Journal of Theoretical and Applied Finance*, 21(06):1850030.
- Albanese, C., Crépey, S., Hoskinson, R., and Saadeddine, B. (2020). XVA analysis from the balance sheet. Working paper; available at <https://math.maths.univ-evry.fr/crepey/papers/xva-analysis-balance.pdf>.
- Biagini, F., Gnoatto, A., and Oliva, I. (2019). Pricing of counterparty risk and funding with CSA discounting, portfolio effects and initial margin. *arXiv preprint arXiv:1905.11328*.
- Bichuch, M., Capponi, A., and Sturm, S. (2018a). Arbitrage-free XVA. *Mathematical Finance*, 28(2):582–620.
- Bichuch, M., Capponi, A., and Sturm, S. (2018b). Robust XVA. *arXiv preprint arXiv:1808.04908*.
- Bielecki, T. and Rutkowski, M. (2004). *Credit Risk: Modeling, Valuation and Hedging*. Springer, Berlin, New York.
- Bielecki, T. and Rutkowski, M. (2015). Valuation and hedging of contracts with funding costs and collateralization. *SIAM Journal of Financial Mathematics*, 6(1):594–655.
- Brigo, D., Buescu, C., Francischello, M., Pallavicini, A., and Rutkowski, M. (2018). Risk-neutral valuation under differential funding costs, defaults and collateralization. *arXiv preprint arXiv:1802.10228*.
- Brigo, D., Capponi, A., and Pallavicini, A. (2014). Arbitrage-free bilateral counterparty risk valuation under collateralization and application to credit default swaps. *Mathematical Finance*, 24(1):125–146.
- Brigo, D. and Masetti, M. (2005). Risk neutral pricing of counterparty risk. In Pykhtin, M., editor, *Counterparty Credit Risk Modeling: Risk Management, Pricing and Regulation*. Risk Books, London.
- Brigo, D., Morini, M., and Pallavicini, A. (2013). *Counterparty Credit Risk, Collateral and Funding*. Wiley Finance. Wiley, Chichester.
- Brigo, D. and Pallavicini, A. (2014). Nonlinear consistent valuation of CCP cleared or CSA bilateral trades with initial margins under credit, funding and wrong-way risks. *Journal of Financial Engineering*, 01(01):1450001.
- Brigo, D., Pallavicini, A., and Papatheodorou, V. (2011). Arbitrage-free valuation of bilateral counterparty risk for interest-rate products: Impact of volatilities and correlations. *International Journal of Theoretical and Applied Finance*, 14(06):773–802.
- Broadie, M., Du, Y., and Moallemi, C. (2011). Efficient risk estimation via nested sequential simulation. *Management Science*.
- Broadie, M., Du, Y., and Moallemi, C. (2015). Risk estimation via regression. *Operations Research*.
- Burgard, C. and Kjaer, M. (2011a). In the balance. *Risk*, November:72–75.

- Burgard, C. and Kjaer, M. (2011b). Partial differential equation representations of derivatives with bilateral counterparty risk and funding costs. The Journal of Credit Risk, 7(3):1–19.
- Capriotti, L., Jiang, Y., and Macrina, A. (2017). AAD and least-square Monte Carlo: Fast Bermudan-style options and XVA Greeks. Algorithmic Finance, 6(1-2):35–49.
- Cherubini, U. (2005). Counterparty risk in derivatives and collateral policies: The replicating portfolio approach. In Tilman, L., editor, ALM of Financial Institutions. Institutional Investor Books.
- Crépey, S. (2015a). Bilateral counterparty risk under funding constraints – Part I: Pricing. Mathematical Finance, 25(1):1–22.
- Crépey, S. (2015b). Bilateral counterparty risk under funding constraints – Part II: CVA. Mathematical Finance, 25(1):23–50.
- Crépey, S., Bielecki, T. S., and Brigo, D. (2014). Counterparty risk and funding: a tale of two puzzles, volume 31 of Chapman and Hall/CRC Press Series in Financial Mathematics. Chapman and Hall/CRC, Boca Raton.
- Crépey, S., Hoskinson, R., and Saadeddine, B. (2019). Balance sheet XVA by deep learning and GPU. Working paper; available at <https://math.maths.univ-evry.fr/crepey/papers/xva-analysis-balance.pdf>.
- Cybenko, G. (1989). Approximations by superpositions of sigmoidal functions. Mathematics of Control, Signals, and Systems, 2(4):303–314.
- de Graaf, C., Feng, Q., Kandhai, B. D., and Oosterlee, C. (2014). Efficient computation of exposure profiles for counterparty credit risk. International Journal of Theoretical and Applied Finance, 17(4).
- de Graaf, C., Kandhai, B. D., and Reisinger, C. (2018). Efficient exposure computation by risk factor decomposition. Quantitative Finance, 18(10):1657–1678.
- Delong, L. (2017). Backward Stochastic Differential Equations with Jumps and Their Actuarial and Financial Applications. Springer, Berlin, New York.
- Duffie, D. and Huang, M. (1996). Swap rates and credit quality. The Journal of Finance, 51(3):921–949.
- E, W., Han, J., and Jentzen, A. (2017). Deep learning-based numerical methods for high-dimensional parabolic partial differential equations and backward stochastic differential equations. Communications in Mathematics and Statistics, 5:349–380.
- El Karoui, N., Peng, S., and Quenez, M. C. (1997). Backward stochastic differential equations in finance. Mathematical Finance, 7(1):1–71.
- Ferguson, R. and Green, A. (2018). Deeply learning derivatives. arXiv preprint arXiv:1809.02233.
- Fries, C. P. (2019). Stochastic automatic differentiation: Automatic differentiation for Monte-Carlo simulations. Quantitative Finance, 19(6):1043–1059.
- Fujii, M., Shimada, A., and Takahashi, A. (2010). Note on construction of multiple swap curves with and without collateral. Available at SSRN:<http://ssrn.com/abstract=1440633>.
- Fujii, M., Shimada, A., and Takahashi, A. (2011). A market model of interest rates with dynamic basis spreads in the presence of collateral and multiple currencies. Wilmott, 54:61–73.
- Fujii, M., Takahashi, A., and Takahashi, M. (2019). Asymptotic expansion as prior knowledge in deep learning method for high dimensional BSDEs. Asia-Pacific Financial Markets, 26(3):391–408.
- Gordy, M. B. and Juneja, S. (2010). Nested simulation in portfolio risk measurement. Management Science, 56(10):1833–1848.
- Green, A. (2015). XVA: Credit, Funding and Capital Valuation Adjustments. Wiley Finance. Wiley, Chichester.
- Gregory, J. (2015). The xVA challenge. Wiley Finance. Wiley, Chichester.

- Han, J. and Long, J. (2018). Convergence of the deep BSDE method for coupled FBSDEs. arXiv preprint arXiv:1811.01165.
- Henry-Labordere, P. (2017). Deep primal-dual algorithm for BSDEs: applications of machine learning to CVA and IM. Available at SSRN:<https://ssrn.com/abstract=3071506>.
- Hornik, K. (1991). Approximation capabilities of multilayer feedforward networks. Neural Networks, 4(2):251–257.
- Huré, C., Pham, H., and Warin, X. (2020). Some machine learning schemes for high-dimensional nonlinear PDEs. Mathematics of Computations, 89:1547–1579.
- Hutzenthaler, M., Jentzen, A., Kruse, T., Nguyen, T. A., and von Wurstemberger, P. (2018). Overcoming the curse of dimensionality in the numerical approximation of semilinear parabolic partial differential equations. arXiv preprint arXiv:1807.01212.
- Ioffe, S. and Szegedy, C. (2015). Batch normalization: Accelerating deep network training by reducing internal covariate shift. Proceeding of the 32nd International Conference on Machine Learning (CML).
- Jentzen, A., Salimova, D., and Welti, T. (2018). A proof that deep artificial neural networks overcome the curse of dimensionality in the numerical approximation of Kolmogorov partial differential equations with constant diffusion and nonlinear drift coefficients. arXiv preprint arXiv:1809.07321.
- Joshi, M. and Kwon, O. (2016). Least squares Monte Carlo credit value adjustment with small and unidirectional bias. International Journal of Theoretical and Applied Finance, 19(8).
- Karlsson, P., Jain, S., and Oosterlee, C. (2016). Counterparty credit exposures for interest rate derivatives using the stochastic grid bundling method. Applied Mathematical Finance, 23(3):175–196.
- Kolmogorov, A. N. (1956). On the representation of continuous functions of several variables by superposition of continuous functions of one variable and addition. Doklady Akademii Nauk SSSR, 108(2):679–681.
- Lichters, R., Stamm, R., and Gallagher, D. (2015). Modern Derivatives Pricing and Credit Exposure Analysis: Theory and Practice of CSA and XVA Pricing, Exposure Simulation and Backtesting. Applied Quantitative Finance. Palgrave Macmillan, London.
- Longstaff, F. A. and Schwartz, E. S. (2001). Valuing American options by simulation: A simple least-squares approach. Review of Financial Studies, 14(1):113–147.
- Pallavicini, A., Perini, D., and Brigo, D. Funding Valuation Adjustment: a consistent framework including CVA, DVA, collateral, netting rules and re-hypothecation. arXiv preprint arXiv:1112.1521.
- Piterbarg, V. (2010). Funding beyond discounting: collateral agreements and derivatives pricing. Risk Magazine, 2:97–102.
- Piterbarg, V. (2012). Cooking with collateral. Risk Magazine, 2:58–63.
- Reisinger, C. and Zhang, Y. (2019). Rectified deep neural networks overcome the curse of dimensionality for nonsmooth value functions in zero-sum games of nonlinear stiff systems. arXiv preprint arXiv:1903.06652.
- Ruf, J. and Wang, W. (2019). Neural networks for option pricing and hedging: a literature review. Available at SSRN:[3486363](https://ssrn.com/abstract=3486363).
- She, J.-H. and Greco, D. (2017). Neural network for CVA: Learning future values. arXiv preprint arXiv:1811.08726.
- Shöftner, R. (2008). On the estimation of credit exposures using regression-based Monte Carlo simulation. The Journal of Credit Risk, 4(4):37–62.

Sokol, A. (2014). Long-Term Portfolio Simulation: For XVA, Limits, Liquidity and Regulatory Capital. Risk Books, London.

(Alessandro Gnoatto) UNIVERSITY OF VERONA, DEPARTMENT OF ECONOMICS,
VIA CANTARANE 24, 37129 VERONA, ITALY
E-mail address, Alessandro Gnoatto: alessandro.gnoatto@univr.it

(Athena Picarelli) UNIVERSITY OF VERONA, DEPARTMENT OF ECONOMICS,
VIA CANTARANE 24, 37129 VERONA, ITALY
E-mail address, Athena Picarelli: athena.picarelli@univr.it

(Christoph Reisinger) OXFORD UNIVERSITY, MATHEMATICAL INSTITUTE
ROQ, WOODSTOCK RD, OXFORD, OX2 6GG, UK
E-mail address, Christoph Reisinger: christoph.reisinger@maths.ox.ac.uk